Aerothermal Loads Measured During Martian Entry of the ExoMars Schiaparelli Lander

A. Gülhan[*], T. Thiele[†], F. Siebe[‡], R. Kronen[§], T. Schleutker[**]

German Aerospace Center (DLR), Cologne, Germany, 51147

The instrumentation package COMARS+ was developed to measure aerothermal parameters on the back cover of the ExoMars Schiaparelli lander during Martian entry. The aerothermal sensors called COMARS combine four discrete sensors measuring static pressure, total heat flux, temperature and radiative heat flux. After passing all acceptance tests, the COMARS+ on the Schiaparelli capsule was launched on top of the Proton launcher on 14th March 2016. All COMARS+ sensors operated nominally during the complete entry phase. But the complete data package is not available due to the anomaly that led to the failure of Schiaparelli shortly before landing. Nevertheless, a subset of the COMARS+ flight data was transmitted real-time during the entry by Schiaparelli and were successfully received by the TGO Orbiter, with the exception of the plasma black-out phase. The measured maximum back cover heat flux rate is approx. 9% of the predicted stagnation point heat flux rate at the front surface stagnation point. Close to the vehicle shoulder on the back cover the radiative heating is up to 61% of the measured total heat flux rate. Measured back cover total heat fluxes are below the sizing total heat flux level of the back cover TPS.

---

[*] Head of the Supersonic and Hypersonic Technologies Department, Institute of Aerodynamics and Flow Technology, Principle Investigator of the COMARS+ Instrumentation Package.

[†] Research Scientist at the Supersonic and Hypersonic Technologies Department, Institute of Aerodynamics and Flow Technology.

[‡] Research Scientist at the Supersonic and Hypersonic Technologies Department, Institute of Aerodynamics and Flow Technology.

[§] Research Engineer at the Supersonic and Hypersonic Technologies Department, Institute of Aerodynamics and Flow Technology.

[**] Research Scientist at the Supersonic and Hypersonic Technologies Department, Institute of Aerodynamics and Flow Technology.

Nomenclature

CFD = Computational Fluid Dynamics

COMARS = Combined Aerothermal and Radiometer Sensor

DHMR = Dry Heat Microbial Reduction

ECSS = European Cooperation for Space Standardization

EDL = Entry, Descent, Landing

EDM = EDL Demonstrator Module

EIP = Entry Interface Point

FADS = Flush Airdata Sensing

HFM = Heat Flux Microsensor of Vatell Company

HFS = Heat Flux Sensor

ICOTOM = Narrow Band Infrared Radiometer

L2K = Arc heated wind tunnel facility of DLR

MCD = Mars Climate Database

PCB = Printed Circuit Board

PSD = Power Spectral Density

SPHF = Stagnation Point Heat flux

TAS-I = Thales Alenia Space Italy

TGO = Trace Gas Orbiter

c_p = pressure coefficient

h = enthalpy, J/kg

M = Mach number

p = pressure, Pa

q = dynamic pressure, Pa

$\dot{q}$ = heat flux rate, $W \cdot m^{-2}$

Re = Reynolds number

St = Stanton number

t = time, s

T = temperature, K

T_0 = total temperature, K

x, y, z = coordinates, m

ρ = density, $kg \cdot m^{-3}$

Subscripts

0 = stagnation condition

∞ = atmospheric (inflow) parameter

meas = measured

w = wall condition

I. Introduction

The first mission of the ExoMars program which arrived at Mars in October 2016, consisted of a Trace Gas Orbiter (TGO) plus an Entry, Descent and Landing Demonstrator Module (EDM) named Schiaparelli. The orbiter and Schiaparelli were launched on 14th March 2016 on a Proton rocket. The main scientific objectives of this mission are to search for evidence of methane and other trace atmospheric gases that could be signatures of active biological or geological processes and to test key technologies in preparation for ESA's contribution to subsequent missions to Mars. Another important objective is the demonstration of a successful entry, descent and landing on Mars. Gathering scientific data during these flight phases is a further key element and would provide very important data for future missions. This data could be used for an optimization of the heat shield, as for example the design of the back cover heat shield was carried out with relatively high safety margins. This is due to the fact that the prediction of the aerothermal and radiative loads on the back cover, using existing experimental and numerical tools, still has big uncertainties.

The first successful mission to Mars including TPS instrumentation was Viking Lander 1 launched in 1975. The pre-flight prediction of the Viking afterbody heating, including a safety factor of 1.5, estimated a value of 3% of the nose laminar heating for the backshell [1][2]. But the Viking post-flight analysis of the temperature data showed that a value of 4.2% was reached. It has to be mentioned that Viking Lander 1 was only instrumented with thin-film

gauges at two locations on the back cover which were spot-welded to aluminum and fiberglass base covers. A heat flux rate of 9.7 kW/m2 was derived from the thermocouple data on the aluminum structure at the time of sensor failure. On the fiberglass cover the sensor worked during the complete entry and a peak heating value of 6.6 kW/m2 was determined [2]. A very interesting finding of this study is the delayed peak heating on the back cover compared to the front shell peak heating. But there is no clear explanation of this behavior.

Very high heat fluxes on the TPS occurred during the Galileo probe entry into the Jovian atmosphere in 1995. The heat shield of the Galileo probe which entered the atmosphere with a relative velocity of 47.4 km/s was exposed to severe heat fluxes up to 170 MW/m2. To measure the TPS recession the capsule was instrumented with Analog Resistance Ablation Detectors (ARAD) and four thermometers [3]. Two thermometers were placed on the back cover and used to predict the rear surface recession based on the front surface recession measured by the ARAD sensors. Because of uncertainties in the front shield data, it was difficult to assess the afterbody heating.

A further successful Mars landing was performed by Mars Pathfinder in 1997 including the first Mars rover. The afterbody frustum of the Mars Pathfinder vehicle was coated with SLA-561S (a spray-on version of SLA-561V). The backshell interface plate and the rear portion of the frustum were covered with SIRCA (Silicone Impregnated Reusable Ceramic Ablator) tiles and had no surface-mounted instrumentation. But the aeroshell did contain nine thermocouples at various depths in the TPS material and three platinum resistance thermometers [4]. Unfortunately some thermocouples failed to provide useable data. For one near-surface thermocouple on the backshell the peak temperature could be matched to the predicted turbulent corner heating scaled by 0.026, but with an incorrect shape of the thermocouple response.

In general the design of the entry capsule is carried out using numerical tools and ground experiments. The aerothermal design and sizing of the TPS of such capsules are carried out using Computational Fluid Dynamics (CFD) codes and ablative material response tools, which are supported by ground experiments. For the design margin of spacecraft structures the reliability of these design tools is essential. Since the physical models in numerical tools can only be validated partially, the design ends at high safety margins, i.e. high mass in the vehicle design. Assumptions like supercatalytic wall, fully turbulent flow environment, strong roughness induced heat flux augmentation, etc. lead to more than 40% extra forebody TPS thickness [5][6], which in turn has a significant impact on the overall mass budget.

Based on this fact the heat shield of the Mars Science Laboratory (MSL), which was launched in 2011 and successfully landed on Mars in 2012, was instrumented with several sensors to acquire important flight data for aerodynamics, aerothermal heating and performance of the TPS [7][8]. The installed MSL sensor package MEDLI (Mars Science Laboratory Entry, Descent, and Landing Instrumentation) allowed collecting pressure, temperature and recession data on the front TPS shield [9].

The MEDLI unit comprises sensors for surface pressure measurements called the Mars Entry Atmospheric Data System (MEADS) and a second instrumentation block for thermal performance (temperature and ablation tracking) of the heat shield called MEDLI Integrated Sensor Plugs (MISP). The MEADS part contains a Flush Airdata Sensing (FADS) system which collects aerodynamic data during flight. The pressure ports are arranged in such a way that aerodynamic parameters (e.g. angle of attack) can be computed from measured pressure values. In addition the measured pressure data allows verification of the trajectory reconstruction algorithm for MSL [10][11]. The MISP is a cylindrical embedded PICA plug with four type-K (chromel-alumel) thermocouples in different depts. In addition to the thermocouples an isotherm following sensor called Hollow aErothermal Ablation and Temperature (HEAT) is also installed in the plug to track the ablation process.

In total seven MISP plugs were installed on the MSL front heat shield and no plugs were installed in the backshell of the vehicle. During Mars entry the MISP temperature data showed the occurrence of boundary-layer transition on the leeward side of the MSL forebody. The data also indicate that the thermal protection system recession was below predicted values.

To determine the overall performance and for trajectory reconstruction the Schiaparelli capsule of the ESA ExoMars 2016 mission was instrumented with four pressure sensors and seven thermal plugs in the front shield [12][13][15].

During former missions investigations concerning TPS heating were mainly focused on the front shield part due to the higher heat loads and less attention was paid to the heat loads on the back cover. An overview of afterbody aeroheating flight data for planetary entry probes is given in the paper of Wright et al. [16]. This paper recommends that for the reduction of mass and risk future planetary entry vehicles should include heat-shield instrumentation. The aftshell is suggested as the safest place to incorporate instrumentation because of the low heating rates.

In contrast to the MSL instrumentation, the Schiaparelli capsule also included several sensors on the back cover. In this region the Reynolds number of the flow is low and the flow itself has a highly transient character which results in comparatively low convective heat fluxes. But the radiative heat flux, mainly resulting from excitation of carbon

dioxide molecules behind the strong bow shock, can be higher, exceeding the convective heat load. But neither ground test facilities nor numerical tools can simulate this radiation environment accurately. In order to close this gap, the Supersonic and Hypersonic Technology Department of the German Aerospace Center (DLR) in Cologne developed the combined aerothermal sensor package COMARS+, based on experience gathered during the flight instrumentation for the flight experiments SHEFEX-I and SHEFEX-II [17][18]. The COMARS+ instrumentation package consists of three combined aerothermal sensors (called COMARS sensors), one broadband radiometer sensor and an electronic box [19]. The aerothermal sensors combine four discrete sensors measuring static pressure, total heat flux, temperature and radiative heat flux at two specific spectral bands. The infrared radiation in a broadband spectral range is measured by the separate broadband radiometer sensor. The electrical interface between sensors and Schiaparelli data handling system is provided by the payload electronic box.

This paper describes the main properties of the COMARS+ payload, mechanical and thermal design details and finally the results of aerothermal tests performed in the arc heated facility L2K at DLR Cologne.

II. Requirements and Design Approach

In the past most capsules for planetary missions had limited instrumentation. In particular the back cover was only instrumented with a minor number of sensors compared to the even limited front shield instrumentation. But, because of its large surface area the back cover of the vehicle has a significant mass impact. To gain reliable flight data and to asses the design margins the COMARS+ instrumentation package was proposed for the Schiaparelli capsule back cover of the ExoMars 2016 mission. At the same time COMARS+ payload had to satisfy a large compliance matrix of requirements with following main constraints:

- COMARS+ may not cause any risk to the success of the mission.
- The total mass of the payload should be less than 2 kg including maturity margins.
- The dimensions shall be as small as possible considering the required fixation points and available envelope.
- The average power consumption should stay below 7 W using an operative voltage between 22 and 36 Volt.

- Qualification tests, acceptance tests and documentation should be performed according to ECSS norm.

These requirements forced DLR to significantly adapt the SHEFEX sensor design and miniaturize sensor heads and electronics [18][19]. During the design phase several thermal and mechanical analyses were performed for verification of the chosen design. Two sets of engineering models were manufactured to verify the preliminary design and general functionality of the components. For the qualification tests a set of qualification models (one COMARS sensor, one broadband radiometer sensor and one electronic box) was manufactured and subjected to mechanical, thermal/vacuum, shock, radiation hardness, electromagnetic compatibility and aerothermal tests at conditions defined by ESA and TAS-I in the applicable requirement documents. In addition to these tests, the cleaning procedure for the planetary protection requirements was tested on the qualification models to demonstrate that the number of spores could be reduced to the necessary level. One set of flight models was manufactured (three COMARS sensors, one broadband radiometer sensor and one electronic box) for the integration into the Schiaparelli capsule. In addition to the flight models a spare part for each individual component was made (one COMARS sensor, one broadband radiometer and one electronic box).

The ExoMars EDM mission (2016) was classified as Planetary Protection Category IVa, being a landed system not carrying life-detection experiments nor accessing a "special region" of Mars. The bioburden constraints for COMARS+ at delivery were defined as:

- Bioburden $\leq$ 1000 bacterial spores on COMARS+ accountable exposed internal and external surfaces.
- Average bioburden density $\leq$300 bacterial spores/m^2 on the COMARS+ accountable exposed internal and external surfaces.
- All COMARS+ harness, including for H/W isolated by H14 equivalent HEPA filters, shall be processed with DHMR using six D-values for encapsulated bioburden.
- The encapsulated spores for COMARS+ payload shall be less than 13200.

To satisfy these requirements all flight and spare components were assembled in a clean room environment and subjected to a bioburden reduction process.

III. Payload Layout

As described in the reference [20] previous combined aerothermal sensors designed for the Shefex-II flight experiment was redesigned to account for different TPS thickness, fixation method, available space and temperature environment. To keep the mass as low as possible, the interface was manufactured from titanium instead of stainless steel. Due to the very low pressure and limited space a different pressure sensor was used. A good compromise was found in a Pirani type pressure sensor which is small and able to measure very low pressures down to a few Pascal. To measure total heat flux and surface temperature, the cabling of the commercial Heat Flux Microsensor (HFM) of Vatell used for SHEFEX-II was slightly adapted to fit into the new sensor interface. Furthermore the sensor interface was extended to incorporate two radiometers which measure the radiative heat flux at two specific spectral bands. These radiometers called ICOTOM were contributed by the French space agency CNES [21] [22]. The infrared radiation in a broadband spectral range was measured by a separate broadband radiometer sensor which was developed for the ExoMars mission. It consists of a thermopile sensor integrated into a titanium sensor interface. To minimize the number of different mechanical interfaces at the back cover, outer dimensions and fixation points of the broadband radiometer interface are identical to the COMARS sensor. The following table presents an overview of the different parts of the COMARS+ instrumentation package.

Table 1 COMARS+ payload overview.

Unit name	Description
Multiplexing Signal Conditioner (MSC)	Electronic box
COMARS1 (COM 1)	Combined static pressure, total heat-flux, temperature and
COMARS2 (COM 2)	two CNES spectral radiometer sensors (ICOTOM)
COMARS3 (COM 3)	
Radiometer (RAD)	Broadband radiometer
Payload harness	Harness connecting the sensors to the electronic box

For the complete payload overall 23 sensor and 8 housekeeping signals have to be amplified to a specified input voltage range and multiplexed to three analogue acquisition channels of the EDM data handling system. This is done using an electronic box which is also part of the payload. In addition to amplification and multiplexing, a sensor signal conditioning is also integrated in the electronic layout. The actual digitization of the sensor signals is done by the capsule onboard data handling system and was not part of the COMARS+ payload. The analogue sensor signals were digitized with a 12 bit resolution and a sampling frequency of 10 Hz.

The location of the three COMARS sensors and the broadband radiometer on the Schiaparelli back cover is shown in Fig. 1.

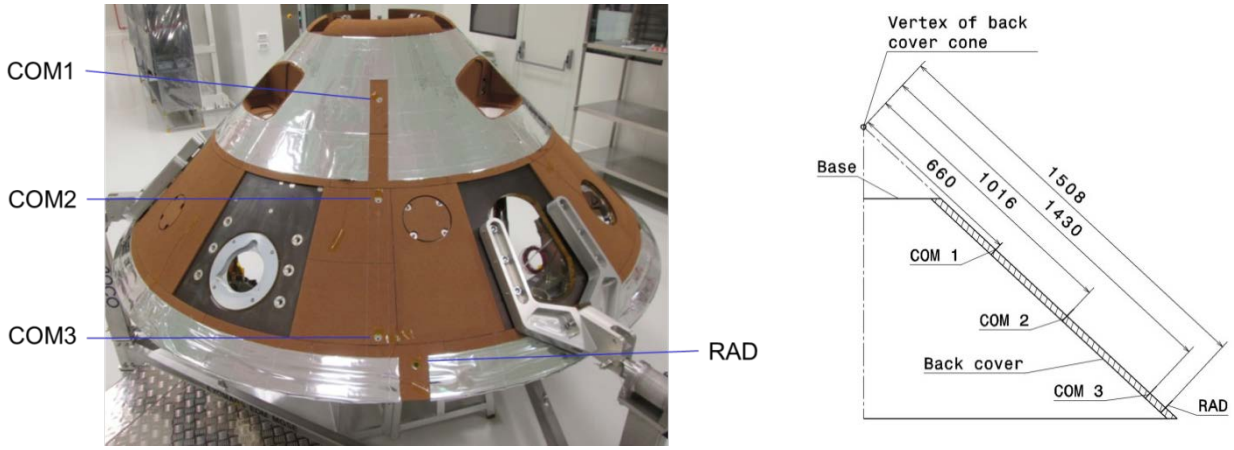

Fig. 1 Position of COMARS+ sensors on the back cover of Schiaparelli.

The COMARS sensors and the broadband radiometer are fixed to the ExoMars back cover structure using honeycomb inserts to which the sensors are screwed with four M4 screws each. Fig. 2 and Fig. 3 show exterior and interior views of the COMARS sensor with denomination of the different parts.

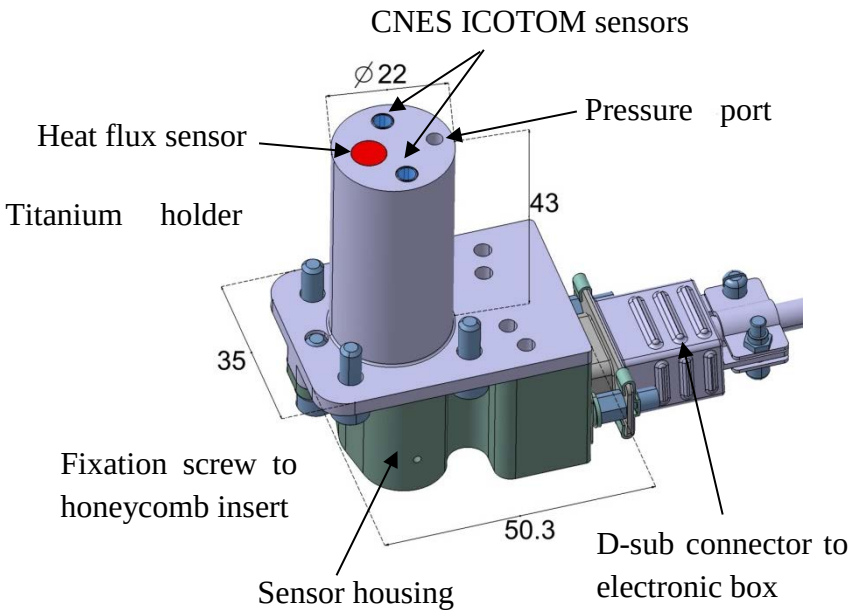

Fig. 2 COMARS sensor assembly top view with dimensions [mm].

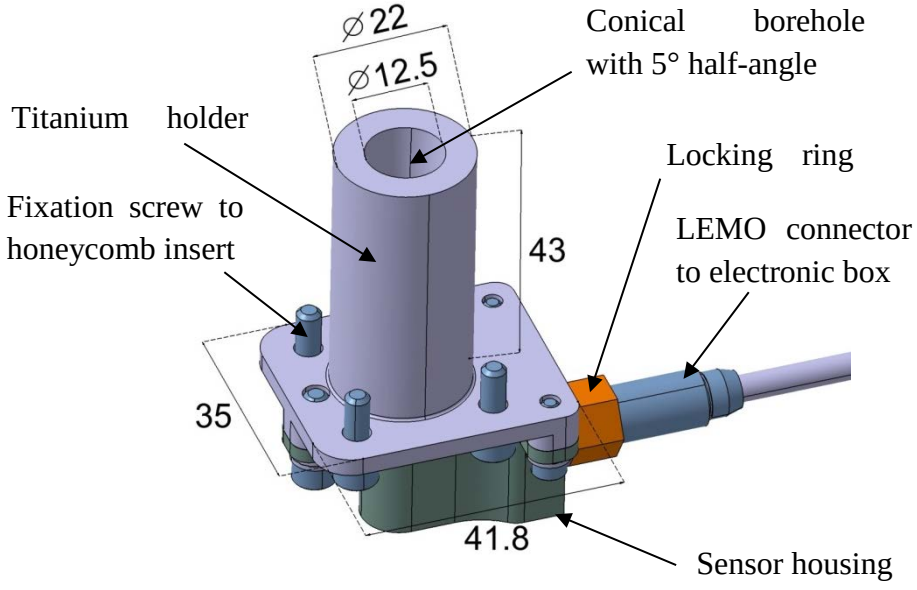

Fig. 3 Broadband radiometer top view with dimensions [mm].

The Multiplexing Signal Conditioner (MSC, COMARS+ electronic box) consists of one multiplexing board and one power board mounted on top of each other in an aluminium housing.. The layout of the Multiplexing Signal Conditioner (MSC, COMARS+ electronic box) is shown in Figure 3. It consists of one multiplexing board and one power board mounted on top of each other in an aluminium housing. The multiplexing board contains amplifiers, filters and the multiplexing circuit for the sensor signals. The power board generates the necessary voltage levels

from the unregulated bus of the EDM using a DC/DC converter. The sensor signal multiplexing is controlled via clock and synchronization signals from the EDM data handling system. More information about the sensors and electronic box is given in the reference [20].

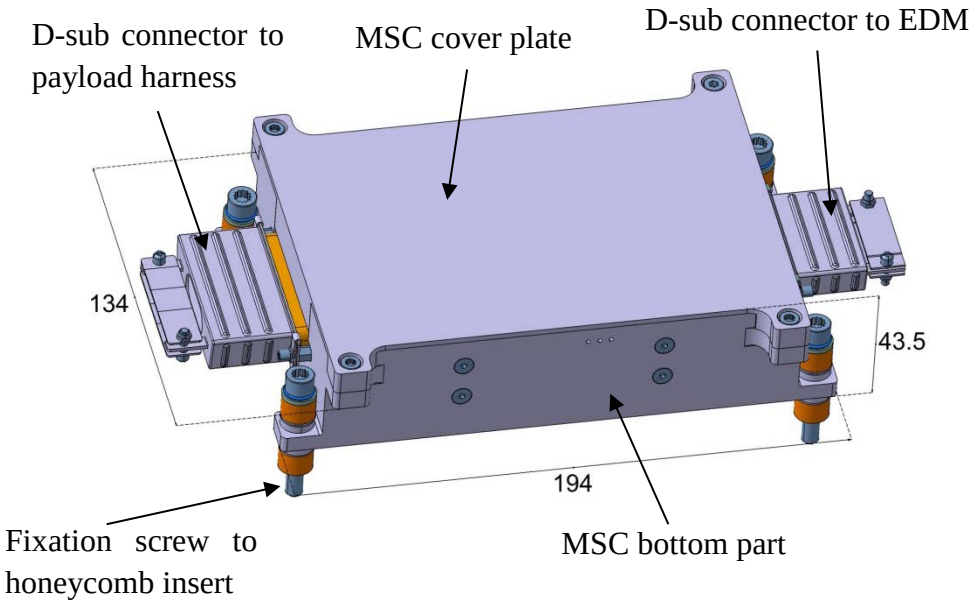

Fig. 4 Electronic box top view with dimensions [mm].

IV. Structural and Thermal Design

A. Structural Analysis

To verify the structural integrity of the COMARS+ components during the launch phase several structural analyses were performed. The electronic box is the heaviest part of the payload with a weight of 920 gram (with margins) and is therefore exposed to the highest mechanical stresses acting on box structure and fixation screws. In the following some results of the numerical analysis for the electronic box are shown. To evaluate the worst case vibration loads during launch and ascent, the qualification random vibration spectra for the electronic box is used (Fig. 5). These random loads are converted into equivalent static loads using the Miles-equation. To do a worst case analysis the amplification factor for the Miles equation is set to Q=16. This is the maximum value measured on the electronic box bottom part during the qualification test campaign resonance search on all three axes. For the simulation this value is used for in-plane and out-of-plane direction. In Fig. 6 a static load curve is plotted for the

complete frequency range between 20-2000 Hz. For the worst case structural analysis the maximum values of 233g (out-of-plane) and 111g (in-plane) are used not taking into account the box natural frequency.

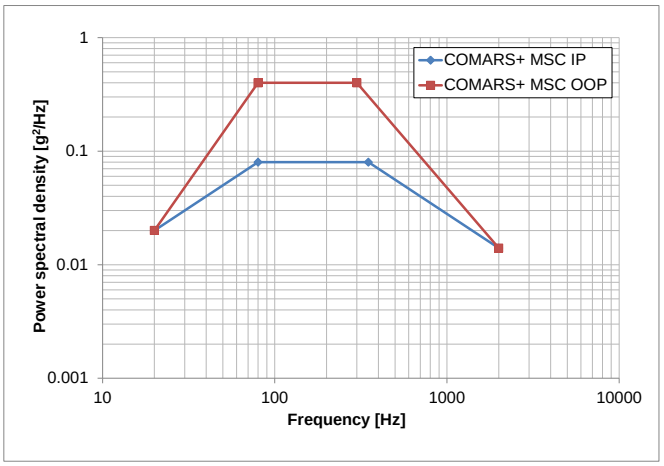

Fig. 5 Random vibration loads of COMARS+ electronic box.

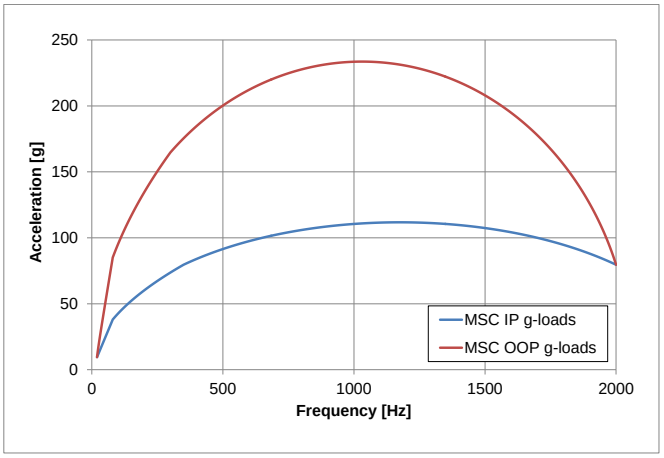

Fig. 6 COMARS+ electronic box static load curve derived from random loads.

For the FEM-model some simplifications were made with respect to detailed interfaces, screws and PCB boards, but the overall mass of the box is kept constant. The resulting von Mises equivalent stress value of 106 MPa for the electronic box occurring at the mounting feet was well below the yield strength of the used aluminium material (380 MPa). The calculated stresses for the fixation components (screws, spacers, thermal washers) were also well inside the corresponding material stress limits. In addition to the structural analyses modal analyses were also performed for sensors and electronic box to determine the first fundamental frequencies. The results showed, that all

fundamental frequencies are above the limit frequency of 140 Hz specified in the ExoMars mechanical interface requirements.

To determine the maximum deflection of the PCBs inside the electronic box a Power Spectral Density (PSD) analysis was performed using the random vibration loads shown in Fig. 5 and a scaling factor of 3 Sigma. Fig. 7 shows the deflection of multiplexing and power board perpendicular to the board plane. The maximum deflection of the multiplexing board occurs around the center. As a fixation screw is placed in the center of the PCB, the deflection is very small with a maximum of 0.2 mm which is well inside the tolerable range. The maximum deflection of the power board is larger with a maximum of 1.0 mm at the short sides. This is because the power board is not fixed to the electronic box structure by D-Sub connectors at these sides. As the components on the power board (DC/DC converter, voltage filter) are placed around the center of the PCB, where the deflections are lower, and are additionally fixed with epoxy adhesive, the larger deflection of the power board is not an issue.

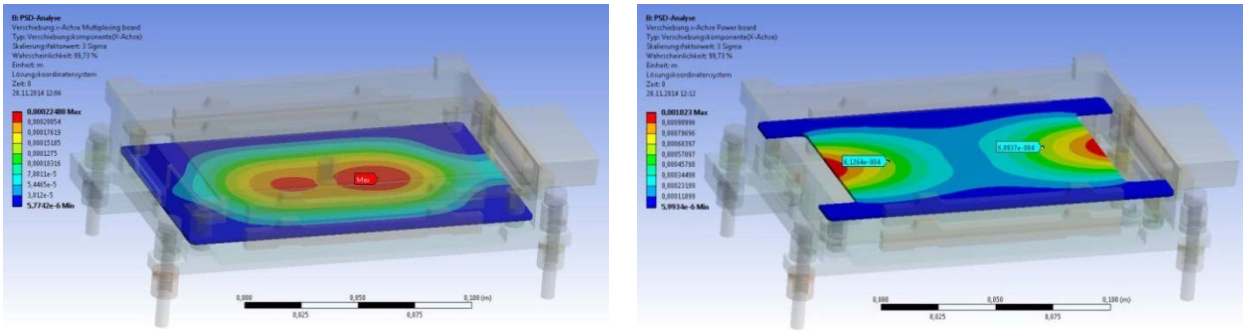

Fig. 7 PSD analysis for electronic box, deflection of multiplexing board (left) and power board (right).

B. Thermal Analysis

To verify the temperature resistance of the COMARS sensor assembly during Mars entry transient thermal analyses were performed. The thermal model consists of a cut-out of TPS and honeycomb structure with integrated COMARS sensor. The honeycomb structure is thereby modelled as a solid structure with adjusted material properties (density, thermal conductivity, specific heat capacity). For the COMARS sensor some simplifications are made for the thermal model. The honeycomb fixation screws, the sensor housing and the D-Sub connector are neglected, as these parts are located at the back end of the sensor and do not influence the heat conduction from the TPS to the lower parts of the sensor. Furthermore the Pirani pressure sensor and the ICOTOM detectors are not incorporated in the thermal model as their thermal properties and inner layout are unknown. Because these parts are

also located at the sensor back end, their influence on the thermal analysis is insignificant. To evaluate the temperatures of Pirani pressure sensor and ICOTOM detectors, the temperature of the corresponding contact surface on the titanium holder is calculated. For the overall thermal model all contacts between the different parts are assumed to be bonded contacts.

The COMARS and broadband radiometer sensors are thereby located in zones V and VI according to Figure 7. The heat flux used for the thermal simulation can be seen in Figure 7 and is taken from the ExoMars EDM aerothermodynamic database.

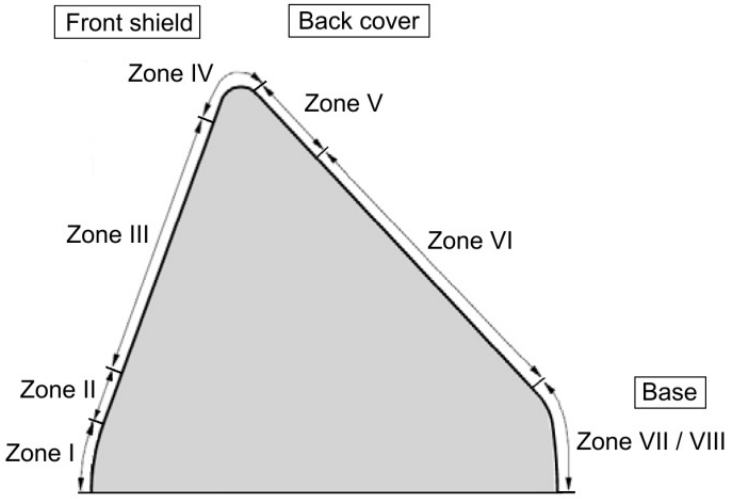

Fig. 8 Zone definition of the Schiaparelli capsule.

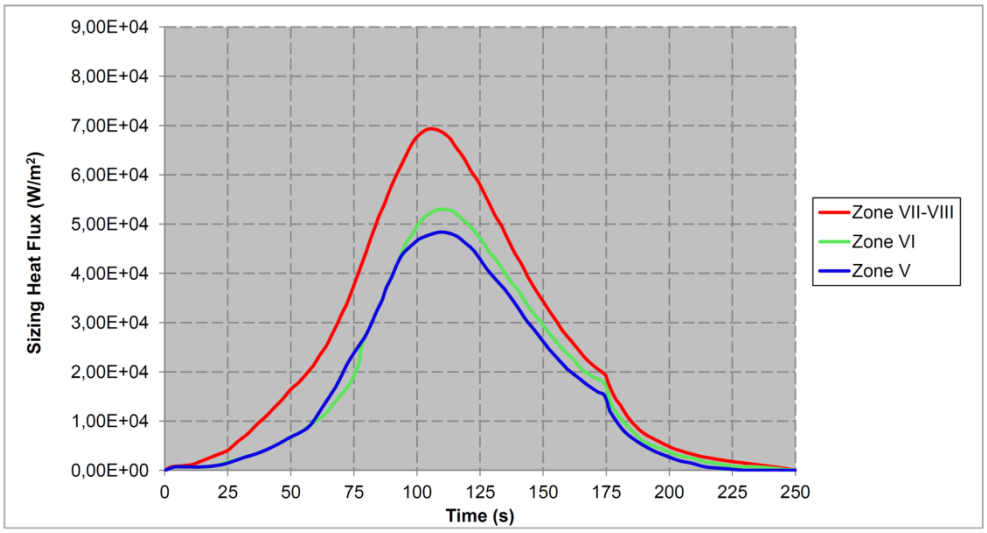

Fig. 9 Sizing heat flux profile for EDM back cover TPS [23].

The heat flux profiles were computed with a wall temperature of 300 K and represent the worst-case heat fluxes to the TPS (sizing case). As the heat flux in zone VI is slightly higher than in zone V, the heat flux of zone VI is used for the thermal simulations. The heat flux according to Fig. 9 is applied to the upper TPS surface including the COMARS sensor surface. To simulate further heat conduction into the material after the heat flux becomes zero (at t=250s), the simulation time is extended to 450 seconds. A radiation to ambient space with an emissivity of 0.9 is assumed for the TPS surface. All other outer surfaces are set to be adiabatic. A uniform starting temperature of 300 K is used for the simulation to be compliant with the wall temperature assumption used for the heat flux calculation. In Fig. 10 the temperature distribution inside the sensor is shown at the end of the simulation with a nearly homogeneous temperature of about 345 K. The resulting maximum temperatures of the different parts are presented in Fig. 11. The COMARS titanium holder reaches a maximum temperature of 400 K at the sensor front end (TPS side) whereas the contact surfaces for Pirani and ICOTOM sensors only heat up to a maximum of 345 K. As already shown in Fig. 10, all sensor parts are at a nearly homogeneous temperature level at the end of the simulation time.

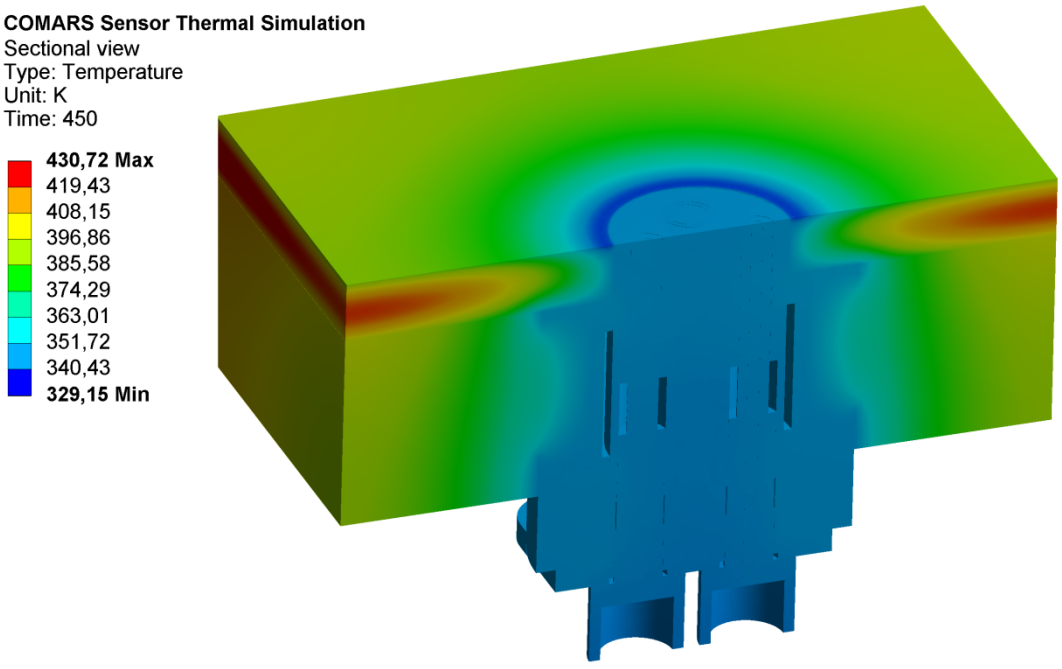

Fig. 10 Computed temperature distribution at the end of simulation the time.

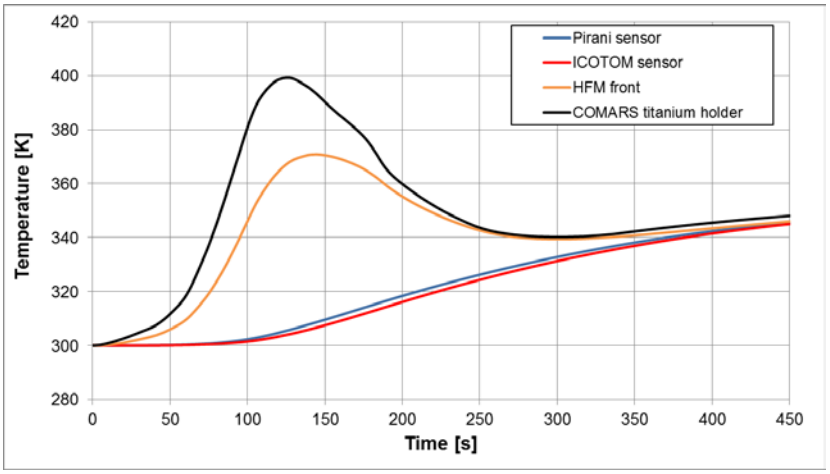

Fig. 11 COMARS sensor thermal simulation maximum temperatures.

In Table 2 calculated temperatures of the COMARS sensor parts are summarized and compared with the corresponding maximum operative range. The EDM back cover separation is assumed to take place around t=320s which is the end of the sensor measurement. Therefore the maximum temperatures before this time point are used for comparison to the maximum operative temperatures. As presented in the table all calculated values are inside the operative range which ensures that the COMARS sensor is capable to withstand the thermal environment during Mars entry.

Table 2 Calculated temperatures compared with maximum operative temperatures for the different COMARS sensor parts.

Part / contact surface	Maximum calculated temperature between t=0s and t=320s [°K]	Maximum operative temperature [°K]
Pirani pressure sensor	335	363
ICOTOM detector	332	348
Heat flux sensor	371	473
COMARS titanium holder	399	673

The calculated temperatures in Table 2 thereby represent worst-case temperatures and the actual values during Mars entry are expected to be lower because of the following reasons:

1. The starting temperature of the different parts will be lower than 300 K at the beginning of Mars entry leading to lower temperatures at the end of the measurement time.

2. The used assumption of bonded contacts between the different parts (perfect heat conduction) leads to higher sensor temperatures.

3. The used heat flux profile taken from the ExoMars EDM aerothermodynamic database represents the back cover TPS sizing case and therefore includes a safety margin.

To verify that the implementation of the COMARS sensor into the TPS will not lead to local overheating of TPS or honeycomb structure, a further simulation was performed only for the TPS structure using the same heat flux levels presented in Fig. 9 Sizing heat flux profile for EDM back cover TPS [23]. A comparison of TPS and honeycomb structure temperatures with and without COMARS sensor showed that the maximum temperatures are lower for the case with a COMARS sensor due to a local heat sink effect. Therefore the integration of the COMARS sensor into the TPS does not cause local overheating of TPS or honeycomb structure. The same is true for the broadband radiometer.

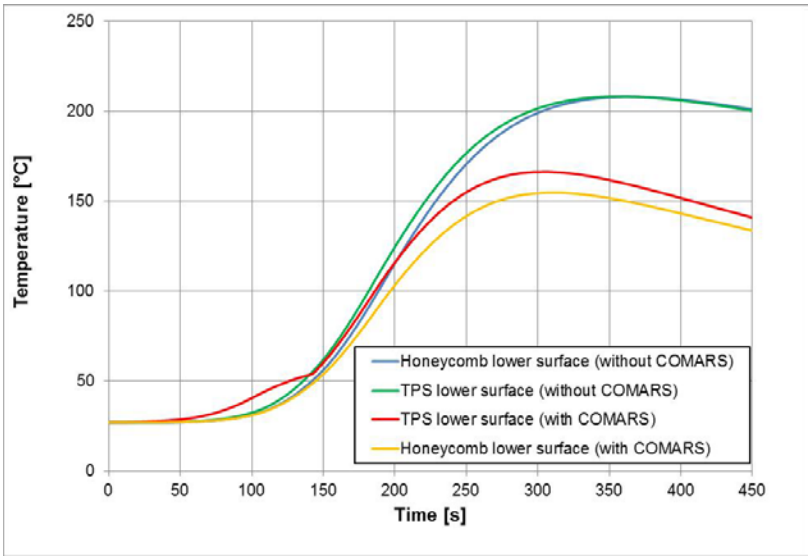

Fig. 12 TPS maximum temperatures with and without COMARS+ sensor.

Another critical parameter is the temperature of the electronic box components during the long cruise phase. Therefore a transient thermal simulation was performed for the electronic box using conductive and radiative heat sink temperatures (thermal environment inside the Schiaparelli) provided by Thales Alenia Space Italy (TAS-I). A homogeneous starting temperature of 235°K and an adaptive time stepping with a maximum time step of 4000 seconds are used for the simulation. The calculated minimum and maximum temperatures for the PCBs inside the electronic box (multiplexing and power board) are shown in Fig. 11. The identical maximum and minimum temperatures indicate that the box is in temperature equilibrium nearly the complete time. The only deviation occurs

at the end of the calculation after the EDL entry point where the Mars entry takes place. At that time, beside the temperature rise due to Mars entry, the box is in its operational state dissipating energy. Because of this transient temperature environment the maximum and minimum temperatures are no longer identical. Although the calculations show that the box temperatures remain well above the minimum non-operative / operative temperatures of about 218°K, TAS-I installed a heater foil on the box casing to heat up the box in case of need.

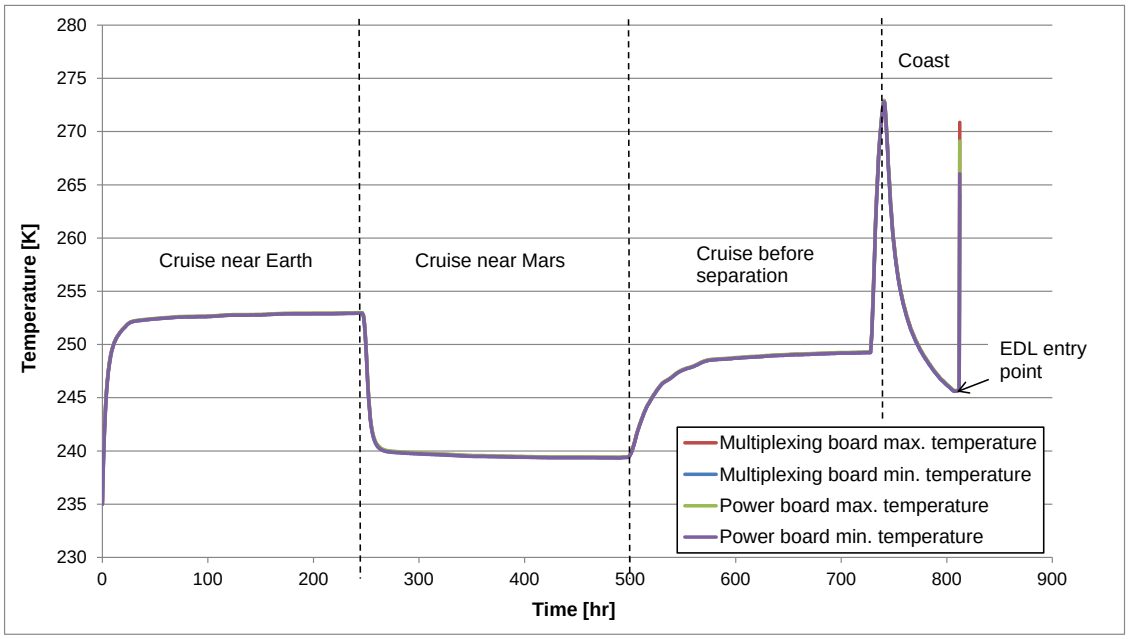

Fig. 13 Electronic box PCBs maximum and minimum temperatures during ExoMars flight.

V. Qualification and Acceptance Tests

The structural and thermal simulations described before were performed as worst case analyses. No verification of the simulation results was performed by tests since the applied mechanical and thermal loads are well oversized, in addition to the simplified boundary conditions which also represent “oversized” assumptions. Therefore the effect of inaccurate numerical modelling can be neglected for these worst case analyses. The design verification was done by extensive qualification and acceptance test campaigns. These tests included:

1. Vibration and shock tests to simulate all mechanical loads that occur during flight, like launch loads and stage separation shocks.
2. Thermal cycling tests under vacuum condition to simulate the thermal environment of the capsule.

3. Electromagnetic compatibility (EMC) tests to check that the payload is compatible with the electromagnetic environment of the capsule and does not emit electromagnetic energy that could cause electromagnetic interference in other devices.
4. Radiation tests for the COMARS+ sensors to verify their radiation hardness.
5. Bioburden reduction and analyses to show the compliance with the planetary protection requirements.

For the qualification tests a set of COMARS+ components was manufactured. These components had to pass all environmental tests listed above. Although the verification of the planetary protection requirements is not necessary for the qualification models, it was necessary to test the cleaning and bioburden reduction approach before applying it on the flight hardware. All qualification tests were performed successfully without any failures or malfunctions. Therefore no design updates were necessary between qualification and flight model. The flight and flight spare models were qualified according to the acceptance test procedures incorporating mechanical, thermal/vacuum and electromagnetic compatibility tests at acceptance level.

To satisfy the requirements concerning planetary protection all flight and flight spare model components and the necessary assembly tools were cleaned thoroughly with Isopropanol before assembly using sterile wipes and an ultrasonic cleaner filled with Isopropanol. Cleaning and assembly were carried out in an ISO 5 laminar flow bench. Afterwards all acceptance tests for the payload parts were conducted in a clean room environment of ISO 8. After successful completion of the tests, all accessible surfaces were again cleaned with Isopropanol. In the final step all payload components except ICOTOM sensors, whose application temperature is limited to 75°C (348 K), were subjected to Dry Heat Microbial Reduction (DHMR) at 122°C for 126 minutes (harness) and 166 minutes (other payload components). The temperature and time periods correspond to a 3-log surface bioburden reduction for the harness cables and a 2-log mated bioburden reduction for the payload components. After DHMR the payload components were brought to a highly controlled ISO 1 clean room for a final functional check. The resulting bioburden of the COMARS+ payload was verified by several bioburden assays taken before the DHMR process and after the final functional test. Overall 22 samples were taken prior to DHMR and 9 samples after the functional test. All assays showed no colony forming units after 72 h of incubation which satisfied the corresponding requirements for surface bioburden. Because the applied conditions for temperature and time during the DHMR process did not reduce the encapsulated bioburden of the COMARS+ hardware, the number of encapsulated spores was evaluated

using bioburden level estimates for flight hardware according to the planetary protection requirements document. Considering the complete volume of the non-metallic payload components, the overall number of encapsulated spores amounts to 7096 which also satisfied the corresponding requirement.

After the final functional test and the verification of the planetary protection requirements the payload components were packed in sterile bags and sent to TAS-I for integration into the Schiaparelli capsule.

Aerothermal tests were performed in the L2K facility of the Supersonic and Hypersonic Technology Department of DLR Cologne [24]. For the final aerothermal tests a representative wedge configuration with integrated qualification models was used [20]. This configuration is similar to the flight case. As during the actual Mars entry, the sensors are directly exposed to boundary layer flow and radiation coming from the shock layer. The COMARS sensor and the broadband radiometer were integrated into the wind tunnel model at the same distance from the model holder nose tip to guarantee the same flow condition on both sensors. The test conditions were chosen in such a way, that the concentration of the CO2 molecules, i.e. radiative heating, could be varied significantly. The enthalpy was varied from 5.6 MJ/kg to 9.2 MJ/kg leading to a CO2 mole fraction change from 0.546 to 0.227. Details description of the tests and results is given in the reference [20].

VI. Flight Data

As reported in several references [14][15] the main data package of the ExoMars EDL phase was stored on board, but part of the data were transmitted to the TGO via telemetry at a low data rate. The data frequency of the transmitted COMARS+ data was 0.1 Hz. The characteristics of the trajectory points at which COMARS+ data was transmitted, as estimated on the basis of Level-0 post flight analyses, are given in Table 3 (values according to private communication with Stefano Portigliotti from TAS-I). The first measurement point S1corresponds to 35 s after the Entry Interface Point (EIP), which is defined as the flight time point with measurable deceleration at 120 km altitude. Although the vehicle velocity of 5829 m/s is very high, the dynamic pressure is quite low due to the low density at an altitude of 82 km. Therefore, as it will be shown later, the aerothermal heating on the back cover is negligible. Because of an approx. one minute communication black out phase the next COMARS+ data was taken at a flight time point of 115 seconds (point S2). At this point the vehicle is already decelerated to a velocity of 2595 m/s at an altitude of 28 km. Corresponding dynamic pressure and Mach number are 5193 Pa and 11.66, respectively.

Atmospheric parameters are derived using MCD v4.3 by LMD Martian atmospheric model, relying atmosphere optical depth for the arrival date derived on the basis of NASA obervations as well as trajectory reconstruction best estimates. The last trajectory point S10 is a few seconds ahead of the parachute deployment.

Table 3 Trajectory points with available COMARS+ flight data.

	Flight time from EIP	Altitude above ground	Aerodynamic speed	Atmospheric density	Atmospheric pressure	Atmospheric temperature	Mach number	Dynamic pressure
	[s]	[km]	[m/s]	[kg/m3]	[Pa]	[K]	[-]	[Pa]
S1	35.553	82.467	5829.38	5.092E-06	0.16	165.50	27.946	86.53
BL								
S2	115.553	28.202	2595.41	1.542E-03	56.56	191.58	11.665	5193.40
S3	125.551	25.477	2013.84	1.979E-03	74.13	195.38	8.967	4013.02
S4	135.552	23.064	1570.58	2.440E-03	93.15	199.13	6.935	3009.56
S5	145.551	20.862	1236.92	2.962E-03	114.57	202.28	5.431	2265.92
S6	155.551	18.887	1001.92	3.478E-03	137.21	205.79	4.360	1745.64
S7	165.553	16.959	823.09	4.078E-03	163.84	209.69	3.553	1381.21
S8	175.551	15.099	685.40	4.751E-03	194.15	213.67	2.937	1115.89
S9	185.552	13.227	584.38	5.496E-03	228.85	217.40	2.483	938.40
S10	195.551	11.379	503.09	6.355E-03	269.55	221.63	2.120	804.24

Measured housing temperature of the COMARS pressure sensors was significantly lower than expected. For the design of the instrumentation sensor structure temperatures between 273 K and 323 K were assumed. But as shown in Fig. 14 the temperatures of the sensor housings were around 245 K with a very slight increase over the measurement time. The temperature of COMARS3 was transmitted as part of the electronic box housekeeping data at lower sampling frequency because of limitations in the number of acquisition channels of the COMARS+ electronic box. It was therefore not included in the reduced data package which was transmitted during Mars entry via TGO. Therefore the temperature of COMARS3 shown in Fig. 14 is the calculated average of COMARS1 and COMARS2 temperatures.

Since the calibration of the radiometer and pressure sensors depends also on the housing temperature, i.e. detector temperature, COMARS+ spare sensors were re-calibrated after the flight at an extended temperature range from 243

K to 323 K. This procedure also allowed checking the repeatability of the pre-flight calibration after the spare sensors were stored in sterilized bags for almost two years. The data reduction of all sensors was carried out using the relation between pre-flight and post-flight calibration data.

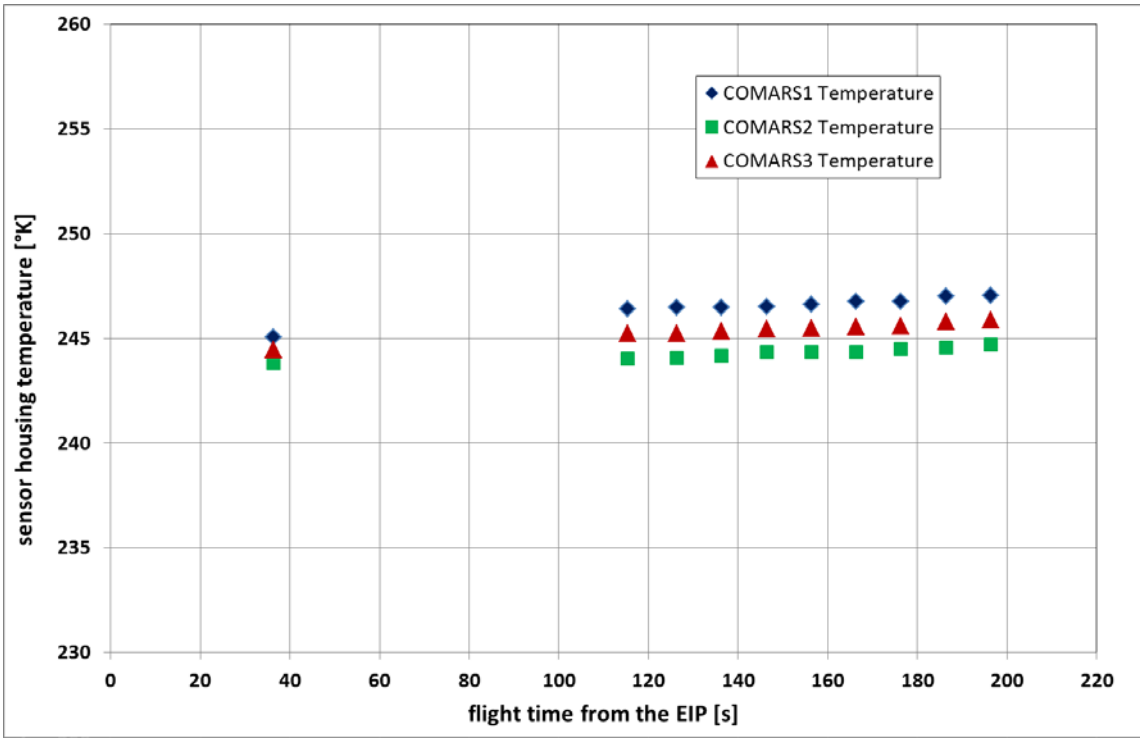

Fig. 14 Measured sensor housing temperatures of COMARS1 and COMARS2 sensors during Schiaparelli entry flight and calculated COMARS3 temperature as the average value of the other two signals.

The measured pressure history of the three COMARS sensors along the trajectory is shown in Fig. 15. All three sensors, which have a measurement uncertainty of ± 5%, measured almost the same pressure level. This behaviour with almost no pressure gradient can be explained with separated flow on the back cover of the capsule. The maximum pressure at the trajectory point S2 is 146 Pa. The predicted dynamic pressure for flight point S2 is approx. 5193 Pa. The pressure coefficient c_p, which is defined as the ratio of the difference between surface pressure (measured COMARS pressure) and free stream atmospheric pressure and dynamic pressure of the free stream (see Eq. 1), is 0.017. The pressure coefficient at the front shield stagnation point, evaluated using preliminary CFD computations, is calculated to 1.929. This means that the surface pressure close to the shoulder on the back cover is approx. 0.9% of the front shield stagnation point pressure.

$$c_p = \frac{p_{meas} - p_\infty}{q_\infty} \qquad (1)$$

If we consider that the peak value of back cover in-depth temperatures measured with thermocouples close to the surface occurs significantly later than the black-out phase [15], measured pressure data should not be far from the peak pressure on the back cover. Until a flight time point of 170 s from the EIP the decreasing surface pressure corresponds well to the dynamic pressure evolution (see Table 3). After this point an increase of the surface pressure is observed. One explanation for this behaviour could be a change of the flow regime in the wake. From earlier studies it is known that depending on Reynolds number and front surface roughness the wake flow may change from laminar to turbulent regime [25]. This leads to a shorter wake, which influences the dynamic stability in a negative way and can cause an increase of the base pressure. Unfortunately there was no base pressure measurement to confirm this assumption.

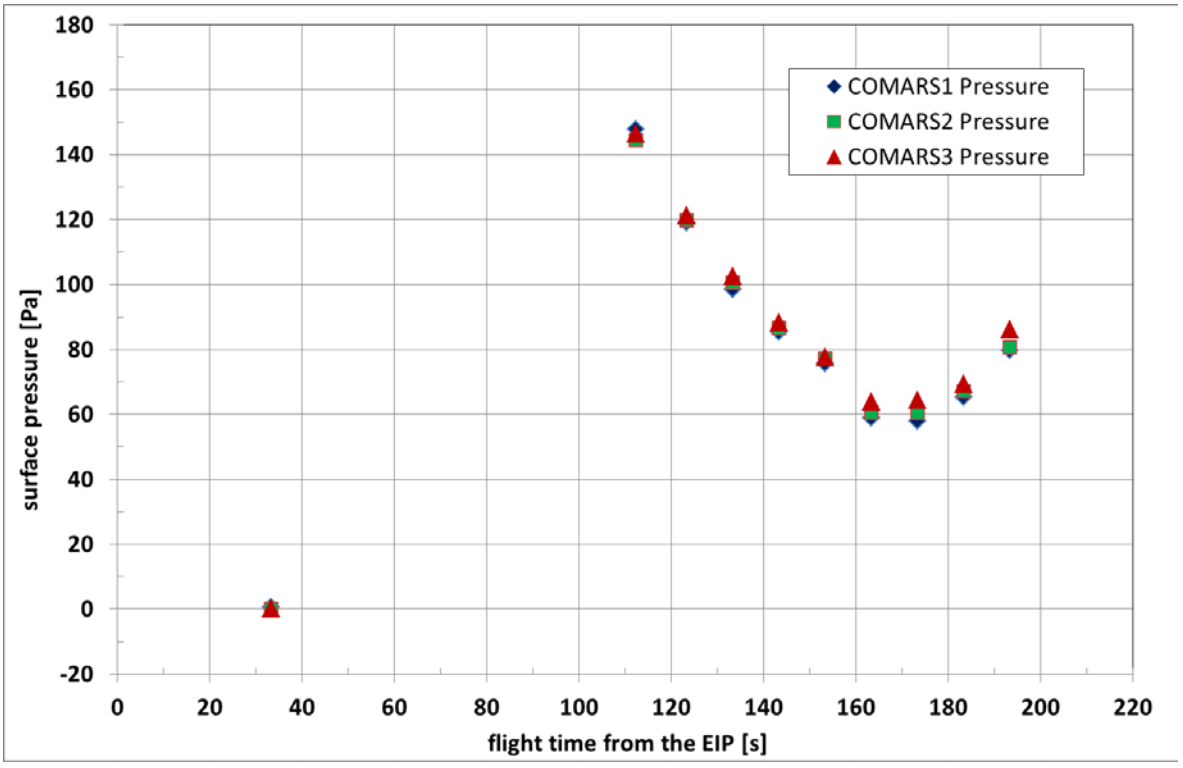

Fig. 15 Measured back cover surface pressure during Schiaparelli entry flight.

Corresponding pressure coefficient values measured with COMARS3, COMARS2 and COMARS1 sensors at trajectory points S2, S3 and S4 are listed in Table 4.

Table 4 Pressure coefficients at the locations of the COMARS sensors at trajectory points S2, S3 and S4.

TP	c_{p3}	c_{p2}	c_{p1}
S2	0.017221	0.017029	0.017606
S3	0.011677	0.011178	0.012924
S4	0.002927	0.002262	0.001597

As mentioned before the total heat flux rate was measured with HFM sensors. A dedicated calibration check was carried out after the flight at low sensor housing temperatures using the COMARS spare sensor. The COMARS3 sensor, located close to the back cover shoulder, measured significantly higher heat fluxes compared to sensors COMARS1 and COMARS2 (see Fig. 2 and Fig. 16) with maximum values of 14.8 kW/m^2, 5.6 kW/m^2 and 2.8 kW/m^2 at trajectory points S2, S3 and S4. For the same trajectory points COMARS2 measured heat fluxes of 11.3 kW/m^2, 3.4 kW/m^2 and 2.2 kW/m^2. Corresponding values of COMARS1 are 11.3 kW/m^2, 4.4 kW/m^2 and 1.4 kW/m^2. It is interesting to see that at trajectory point S3 COMARS1 measures a higher value than COMARS2. At this moment there is no explanation for this behaviour, but it has to be mentioned that the uncertainty of the heat flux measurement is ±8% and the base flow is highly unsteady. The heat flux levels at the trajectory points S5 to S10 are too low for a credible assessment.

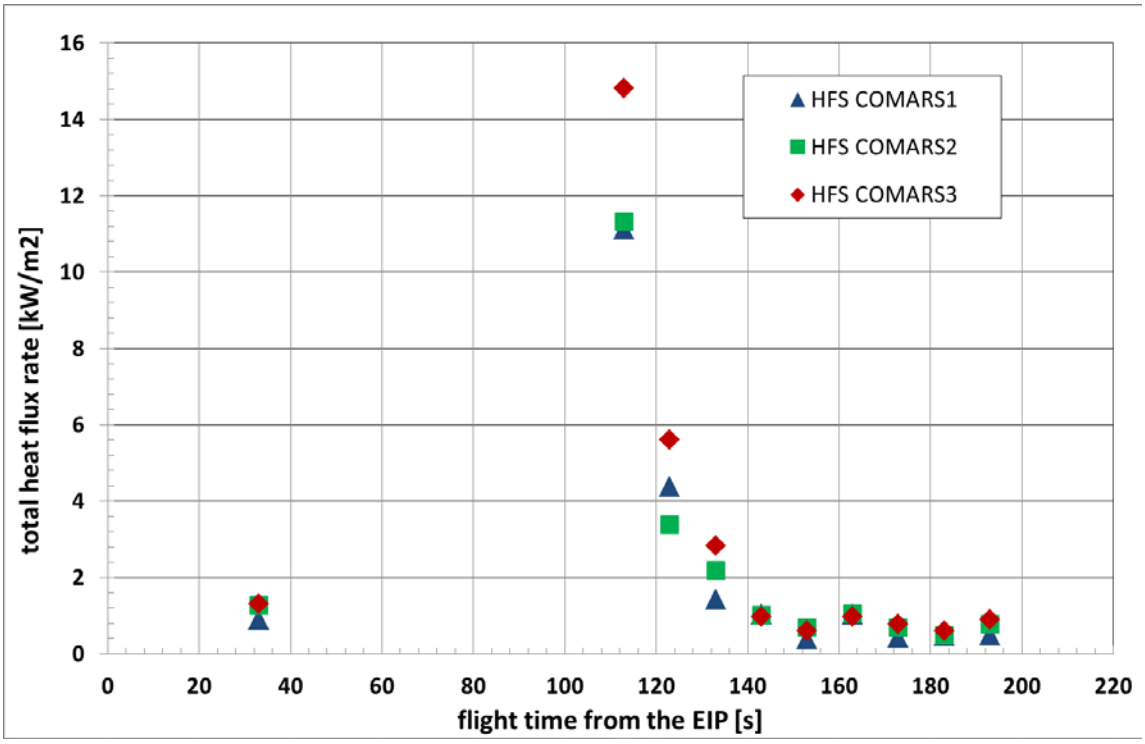

Fig. 16 Measured total heat flux rate on the back cover during Schiaparelli entry flight.

In order to show the relation between measured heat fluxes on the back cover and the total energy of the gas in the shock layer, an evaluation of the Stanton number defined in Eq. 2 has been performed. In this equation the recovery factor is set to 1 and the wall temperature is assumed to be 300 K. Since the heat flux sensor is made out of metal material with a high thermal conductivity and measured structure temperatures are around 245 K (see Fig. 14), this assumption is justified.

$$St = \frac{\dot{q}_{meas}}{\rho_\infty u_\infty (h_0 - h_w)} \qquad (2)$$

As shown before only at trajectory points S2, S3 and S4 measured heat fluxes are high enough to determine any relation to the gas parameters accurately. The calculated Stanton numbers are shown in Table 5. Compared to the front shield stagnation point Stanton numbers of the COMARS3 data at trajectory points S2, S3 and S4, which were determined to 0.001161, 0.000766 and 0.000654, respectively, the back cover values are one order of magnitude lower. It has to be mentioned that for the Stanton number determination free stream atmospheric parameters are used. The use of local boundary layer edge parameters may be a more suitable comparison, but this requires dedicated CFD computations including the simulation of a partially separated wake flow.

Table 5 Stanton number values at the location of the COMARS sensors at trajectory points S2, S3 and S4.

TP	St_{HFS3}	St_{HFS2}	St_{HFS1}
S2	0.001161	0.000886	0.000886
S3	0.000746	0.000453	0.000586
S4	0.000654	0.000514	0.000327

The highest ratio of the heat flux rate measured with COMARS3 to the predicted stagnation point heat flux rate at trajectory point S2 is approx. 0.09. This ratio decreases to approx. 0.06 for trajectory points S3 and S4, respectively. In case of sensors COMARS2 and COMARS1, which are located at a higher distance to the vehicle shoulder, the ratios of the measured heat flux rates to calculated front surface stagnation point heat fluxes are approx. 0.07 at trajectory point S2 and decrease to roughly to 0.04 to 0.05 at trajectory points S3 and S4. Table 6 lists the calculated ratios for the different trajectory points.

Table 6 Ratio of measured back cover heat fluxes and calculated stagnation point heat flux rate.

TP	HFS3/SPHF	HFS2/SPHF	HFS1/SPHF
S2	0.09	0.07	0.07
S3	0.06	0.04	0.05
S4	0.06	0.05	0.03

Fig. 17 shows a comparison between the total heat flux rate of COMARS3 and the radiative heat flux rate measured with the broadband radiometer, which are located very close to each other (Fig. 1). At trajectory point S2 the measured radiative heat flux is 9.0 kW/m^2. The corresponding ratio of radiative heat flux rate to total heat flux rate for trajectory point S2 is therefore 0.61. This ratio decreases to 0.33 and 0.10 for trajectory points S3 and S4, respectively. The measured radiative heat fluxes at trajectory points S1 and S5-S10 are too low for a qualified assessment. The uncertainty of the radiative heat flux measured with the broadband radiometer is in the range of ±15%.

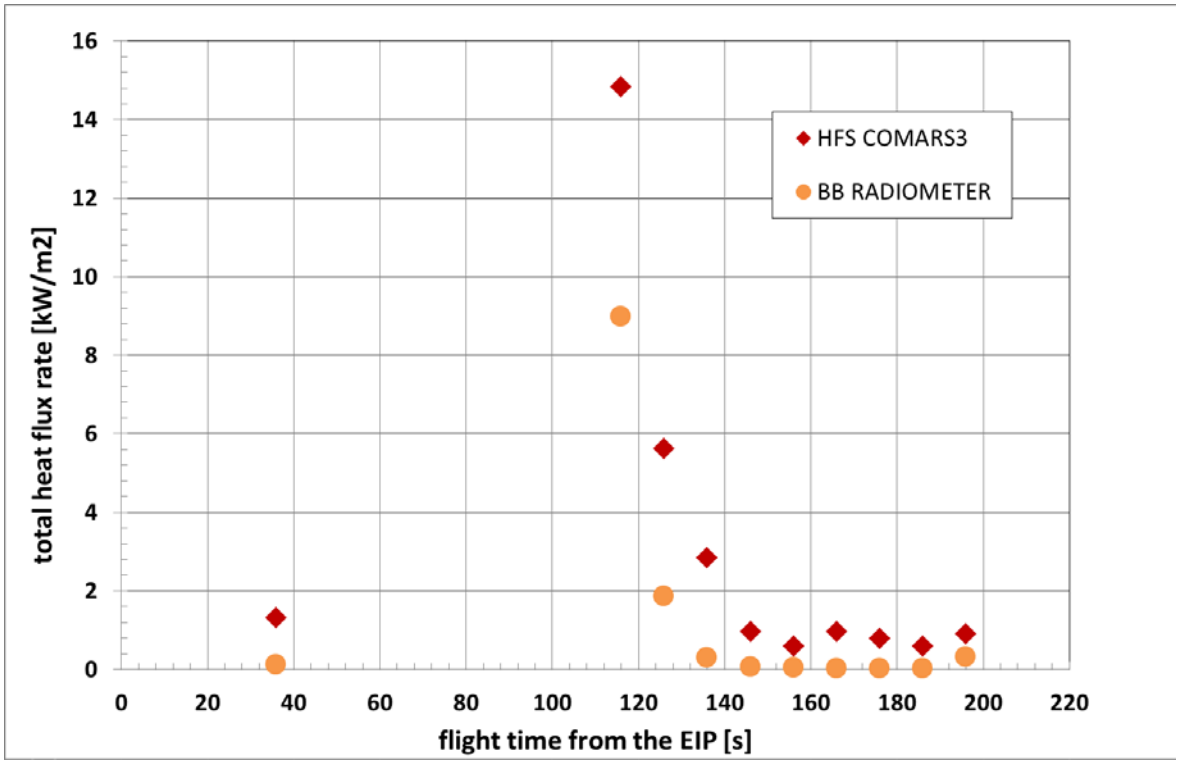

Fig. 17 Measured total heat flux rate and radiative heat flux rate on the back cover during Schiaparelli entry flight.

Another very interesting result is the relation between the radiative and total heat flux. As shown in Table 7 at trajectory point S2 the radiative heat flux rate measured with the broadband radiometer (RAD) is 61% of the total heat flux rate measured with the heat flux sensor HFM3. In the same table the ratio of radiative heat flux to calculated stagnation point heat flux rate (SPHF) is also presented. At trajectory point S2 the specific enthalpy is high enough for the electronic excitation of sufficient CO_2 molecules, which emit radiation by falling from the excited state to the ground level. At trajectory points S3 and S4 the specific enthalpy, i.e. the electronic excitation of CO_2 molecules, is weak or negligible. An important result is the high contribution of radiative heating (61%) to the overall aerothermal heating close to the shoulder region. It decreases with increasing distance from the shoulder [22]. This result is important for the design of back cover TPS. But it has to be mentioned, that measured back cover heat fluxes are far below the sizing total heat flux level of approx. 50 kW/m^2 (Fig. 9) [23].

Since the measurement of the maximum heat flux point of the back cover heat flux profile was not possible due to the black-out phase and the measured front surface heat load profile is missing, the hypothesis that the back cover

heating maximum is delayed with respect to the front shield heating (as mentioned in reference [2]) cannot be confirmed.

Table 7 Ratio of measured radiative heat flux to calculated stagnation point heat flux and measured back cover total heat flux.

TP	BB-RAD/SPHF	BB-RAD/HFS3
S2	0.05	0.61
S3	0.02	0.33
S4	0.01	0.10

VII. Summary and Conclusions

In order to measure aerothermal parameters on the back cover of the ExoMars Schiaparelli lander the instrumentation package COMARS+ consisting of three combined aerothermal sensors, one broadband radiometer sensor and an electronic box was flown on the back cover of the ExoMars Schiaparelli capsule. The aerothermal sensors called COMARS combined four discrete sensors measuring static pressure, total heat flux, temperature and radiative heat flux at two specific spectral bands. The infrared radiation in a broadband spectral range was measured by the separate broadband radiometer sensor. The electronic box of the payload was used for amplification, conditioning and multiplexing of the sensor signals. The ambitious low mass and low power design ended with a total mass of 1.73 kg and a power consumption of 4.5 Watt for the complete payload.

Although the landing of Schiaparelli failed, a part of the flight data during the entry phase were transmitted to the TGO at low sampling rate. All COMARS+ sensors delivered useful data with respect to total heat flux rate, radiative heat flux rate, surface temperature and surface pressure of Schiaparelli from the Martian entry point until parachute deployment with the exception of the plasma black-out phase. Since measured structure and sensor housing temperatures were below predicted pre-flight values, a further calibration using the COMARS+ spare sensors at temperatures down to 243 K was conducted. The main results of the COMARS+ in-flight measurements can be summarized as follows:

- Measured surface pressure data show almost no pressure gradient on the back cover. This can be explained with separated flow on the back cover of the capsule. The pressure coefficient measured with sensor COMARS3 close to the vehicle shoulder is 0.017.
- Following a continuous surface pressure decrease phase an unexpected pressure increase was measured. One explanation for this behaviour could be a change of the wake flow from laminar to turbulent regime with an impact on shape and pressure.
- The highest ratio of the heat flux rate, which is measured with COMARS3 close to the vehicle shoulder, to the predicted stagnation point heat flux rate at the trajectory point S2 immediately after the communication black-out is approx. 0.08 and 0.09 for shallow and steep trajectories, respectively. This ratio decreases to approx. 0.07 for the later trajectory points S3 and S4, respectively. In case of the sensors COMARS2 and COMARS1, which are located in bigger distance from the vehicle shoulder, the ratios of the measured heat flux rates to the calculated front surface stagnation point heat fluxes are approx. 0.06 to 0.07 at the trajectory

point S2 and decrease to roughly to 0.04 to 0.05 at the trajectory pints S3 and S4. These results confirm an important radiative contribution of the radiative heating close to the shoulder on the back cover.

- At the first trajectory point after communication black-out (S2) the measured radiative heat flux is 9.0 kW/m^2. This means 61% of radiative heating compared to the total heat flux rate. This value decreases to 34% and 11% for the later trajectory points S3 and S4, respectively. Decreasing velocity, i.e. specific enthalpy of the flow, along the trajectory points leads to reduced excitation of carbon dioxide molecules and weaker radiation.
- Measured back cover total heat fluxes are below the sizing total heat flux level of the back cover TPS. This very important result suggests that the design margins of the back cover TPS design can be reduced.

Acknowledgement

The authors wish to thank Olivier Bayle (ESA) for his significant and continuous support for the implementation of the COMARS+ on-board Schiaparelli and for the decision to transmit a subset of COMARS+ data during the entry phase, and Stefano Portigliotti (TAS-I) for all fruitful technical discussions and his support during the post-flight analysis.

References

[1] Ingoldby, R. N., Michel, F. C., Flaherty, T. M., Doryand, M. G., Preston, B., Villyard, K. W., and Steele, R. D., "Entry Data Analysis for Viking Landers 1 and 2 Final Report," NASA CR-159388, Martian Marietta Corporation, Nov. 1976.

[2] Edquist, K. T., Wright, M. J., and Allen, G., "Viking Afterbody Heating Computations and Comparisons to Flight Data," *44th AIAA Aerospace Sciences Meeting and Exhibit*, AIAA 2006-386, Reno, Nevada, January 2006. doi: 10.2514/6.2006-386

[3] Milos, F. S., "Galileo Probe Heat Shield Ablation Experiment," *Journal of Spacecraft and Rockets*, Vol. 34, No. 6, 2017, pp. 705-713. doi: 10.2514/2.3293

[4] Milos, F. S., Chen, Y.-K., Congdon, W. M., and Thornton, J. M., "Mars Pathfinder Entry Temperature Data, Aerothermal Heating, and Heatshield Material Response," *Journal of Spacecraft and Rockets*, Vol. 36, No. 3, 1999, pp. 380-391. doi: 10.2514/2.3457

[5] Edquist, K. T., Dyakonov, A. A., Wright, M. J., and Tang, C. Y., "Aerothermodynamic Design of the Mars Science Laboratory Heatshield," *41st AIAA Thermophysics Conference*, San Antonio, Texas, 2009.
doi: 10.2514/6.2009-4075

[6] Wright, M. J., Beck, R. A. S., Edquist, K. T., Driver, D., Sepka, S. A., Slimko, E. M., Wilcockson, W. H., DeCaro, A., and Hwang, H. H., "Sizing and Margins Assessment of the Mars Science Laboratory Aeroshell Thermal Protection System," AIAA Paper 2009-4231, June 2009.
doi: 10.2514/6.2009-4231

[7] Little, A., Bose, D., Karlgaard, C., Munk, M., Kuhl, C., Schoenenberger, M., Antill, C., Verhappen, R., Kutty, P., and White, T., "The Mars Science Laboratory (MSL) Entry, Descent and Landing Instrumentation (MEDLI): Hardware Performance and Data Reconstruction," *36th AAS Guidance and Control Conference*, Breckenridge, Colorado, Feb. 2013.

[8] Bose, D., White, T., Santos, J. A., Feldman, J., Mahzari, M., Olson, M., and Laub, B., "Initial Assessment of Mars Science Laboratory Heatshield Instrumentation and Flight Data," AIAA Paper 2013-0908, Jan. 2013.
doi: 10.2514/6.2013-908

[9] Bose, D., White, T., Mahzari, M., and Edquist, K. T., "Reconstruction of Aerothermal Environment and Heat Shield Response of Mars Science Laboratory," *Journal of Spacecraft and Rockets*, Vol. 51, No. 4, 2014, pp. 1174-1184.
doi: 10.2514/1.A32783

[10] Karlgaard, C. D., Kutty, P., Schoenenberger, M., Shidner, J., and Munk, M., "Mars Entry Atmospheric Data System Trajectory Reconstruction Algorithms and Flight Results," AIAA Paper 2013-0028, Jan. 2013.
doi: 10.2514/6.2013-28

[11] Schoenenberger, M., Norman, J. V., Karlgaard, C., Kutty, P., and Way, D., "Assessment of the Reconstructed Aerodynamics of the Mars Science Laboratory Entry Vehicle," *Journal of Spacecraft and Rockets*, Vol.51, No. 4, 2014, pp. 1076-1093.
doi: 10.2514/1.A32794

[12] Bayle, O., Lorenzoni, L. V., Blancquaert, T., Langlois, S., Walloschek, T., Portigliotti, S., and Capuano, M., "ExoMars Entry Descent and Landing Demonstrator Mission and Design Overview," *8th International Planetary Probe Workshop*, Portsmouth, Virginia, June 2011.

[13] Lorenzoni, L. V., "ExoMars 2016 Entry Descent and Landing Overview," *10th International Planetary Probe Workshop*, San Jose, California, June 2013.

[14] Blancquaert, T., Bayle, O., Lorenzoni, L. V., and Ball, A. J.**,** "ExoMars Entry, Descent and Landing Demonstrator Schiaparelli: flight overview and mission results," *14th International Planetary Probe Workshop*, The Hague, The Netherlands, June 2017.

[15] Portigliotti, S., Cassi, C., Montagna, M., Martella, P., Faletra, M., Boi, J., De Sanctis, S., Granà, D., Bayle, O., Blancquaert, T., and Lorenzoni, L., "ExoMars 2016, the Schiaparelli Mission. EDL Demonstration Results from Real Time Telemetry before Unfortunate Impact," *14th International Planetary Probe Workshop*, The Hague, The Netherlands, June 2017.

[16] Wright, M. J., Milos, F. S., and Tran, P., "Afterbody Aeroheating Flight Data for Planetary Probe Thermal Protection System Design," *Journal of Spacecraft and Rockets*, Vol. 43, No. 5, 2006, pp. 929-943. doi: 10.2514/1.17703

[17] Eggers, T., Longo, J., Turner, J., Jung, W., Hörschgen, M., Stamminger, M., Gülhan, A., Siebe, F., Requardt,. G., Laux, T., Reimer, T., and Weihs, H., "The SHEFEX Flight Experiment -Pathfinder Experiment for a Sky Based Test Facility-," *14th AIAA/AHI Space Planes and Hypersonic Systems and Technologies Conference*, Canberra, Australia, Nov. 2006. doi: 10.2514/6.2006-7921

[18] Gülhan, A., Siebe, F., Thiele, T., Neeb, D., Turner, J., and Ettl, J., "Sharp Edge Flight Experiment-II Instrumentation Challenges and Selected Flight Data," *Journal of Spacecraft and Rockets*, Vol. 51, No. 1, 2014, pp. 175-186. doi: 10.2514/1.A32572

[19] Gülhan, A., Thiele, T., and Siebe, F., "Combined Sensor Assembly COMARS+ for ExoMars EDM Demonstrator," *7th European Workshop on Thermal Protection Systems and Hot Structures*, ESA, Noordwijk, The Netherlands, April 2013.

[20] Gülhan, A., Thiele, T., Siebe, F., and Kronen, R., "Combined Instrumentation Package COMARS+ for the ExoMars Schiaparelli Lander," *Space Science Reviews*, Vol. 214, No. 1, Feb. 2018, Doi: 10.1007/s11214-017-0447-4

[21] Omaly, P., and Hebert, P. J., "ICOTOM: Integrated Narrow Band Infrared Radiometer," *11th International Planetary Probe Workshop*, Pasadena, California, June 2014.

[22] Gülhan, A., Thiele, T., Siebe, F., Schleutker, T., Kronen, R., Annaloro, J., Omaly, P., and Hebert, P. J., "Achievements of the COMARS+ Instrumentation Package During the Entry Flight Phase of the ExoMars Schiaparelli Lander," *14th International Planetary Probe Workshop*, The Hague, The Netherlands, June 2017.

[23] Venditto, P., "ExoMars EDM Aerothermodynamic Database (ATDB)," Thales Alenia Space, Internal Document, Issue 7, July 2011.

[24] Gülhan, A., and Esser, B., "Arc-Heated Facilities as a Tool to Study Aerothermodynamic Problems of Re-entry Vehicles," *Advanced Hypersonic Test Facilities*, edited by F. K. Lu and D. E. Marren, Progress in Astronautics and Aeronautics, Vol. 198, AIAA, 2002, pp. 375-403.
doi: 10.2514/5.9781600866678.0375.0403

[25] Gülhan, A., Klevanski, J., and Willems, S., "Experimental Study of the Dynamic Stability of the ExoMars Capsule," *Proceedings of 7th European Symposium on Aerothermodynamics*, ESA SP-692, Brugge, Belgium, May 2011.